5th International Conference on Experimental Fluid Mechanics ICEFM 2018 Munich
Munich, Germany, July 2-4, 2018

Attractors for the motion of finite-size particles in a two-sided anti-parallel lid-driven cavity

Haotian Wu[1*], Francesco Romanò[12], Hendrik Kuhlmann[1]

[1] TU Wien, Institute of Fluid Mechanics and Heat Transfer, 1060 Vienna, Austria

[2] University of Michigan, Department of Biomedical Engineering, Ann Arbor, MI 48109-2099

[*] haotian.wu@tuwien.ac.at

Abstract

The motion of a neutrally-buoyant spherical particle in the incompressible flow in a two-sided lid-driven cavity is investigated experimentally and numerically. Moderate Reynolds numbers are considered for which the flow is steady and three-dimensional. These flows are characterized by a Lagrangian topology for which regular and chaotic streamlines coexist. Attractors for the motion of the neutrally-buoyant particle are found for certain combinations of Reynolds number and particle size.

1 Introduction

A new mechanism for the attraction of finite-size particles to periodic and quasi-periodic orbits in incompressible closed steady flows has been suggested by Hofmann and Kuhlmann (2011). The mechanism is based on particle advection in the bulk and a restricted particle motion near the boundaries.

To demonstrate the general applicability of the concept of Hofmann and Kuhlmann (2011) we investigate the flow and particle motion in a two-sided lid-driven cavity. Upon an increase of the Reynolds number the incompressible flow in the cavity bifurcates from a steady two-dimensional flow (except from end effects) to a steady three-dimensional convective cellular flow which is spatially periodic (Kuhlmann et al., 1997; Albensoeder and Kuhlmann, 2002; Blohm and Kuhlmann, 2002). Within each convective cell, chaotic and regular streamlines coexist. The latter arise in form of Kolmogorov–Arnold–Moser (KAM) tori (Ottino, 1989; Romanò et al., 2017). When a finite-size particle is transported near an indeformable boundary, it experiences strong repulsion forces due to the particle–boundary interaction (Romanò and Kuhlmann, 2016). The lubrication forces, which dominate the particle dynamics near such boundaries, cause a dissipation of part of the kinetic energy of the particle, almost annihilating its velocity normal to the boundary. Owing to this dissipation effect, along with an appropriate combination of Reynolds number and particle size, nearly neutrally-buoyant finite-size particles can be transported efficiently from the region occupied by chaotic streamlines to a region of regular streamlines. Once the particle moves within the regular region, it can be attracted to periodic or quasi-periodic attractors which typically lie inside of a KAM torus (Kuhlmann et al., 2016; Hofmann and Kuhlmann, 2011).

Here we employ three-dimensional particle tracking to measure the trajectory of a single particle. The periodic and quasi-periodic particle motion found is compared with numerical flow structures. Furthermore, the rapid particle attraction is explained on the basis of particle advection in the bulk and the particle–surface interaction model originally proposed by Hofmann and Kuhlmann (2011) and refined by Mukin and Kuhlmann (2013) and Romanò and Kuhlmann (2016).

2 Experiment Setup

A nearly rectangular cavity is realized between two parallel horizontal cylinders with radius $R = 135\,\mathrm{mm}$. The cylinders can rotate independently about their axes with angular velocities $\Omega_1 = \Omega_2 = \Omega$, as shown in Fig. 1. The height and the span of the cavity are, respectively, $H = 40\,\mathrm{mm}$ and $L = 435\,\mathrm{mm}$. The minimum and maximum distance between the moving walls of the cavity are $W_{\min} = 63\,\mathrm{mm}$ and $W_{\max} = 65\,\mathrm{mm}$,

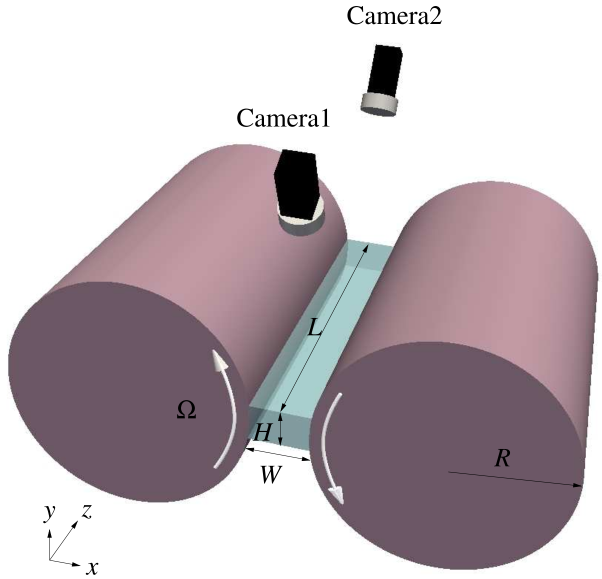

Figure 1: Sketch of the experiment setup and the coordinate system of the cavity. White arrows indicate the direction of rotation of the cylinders.

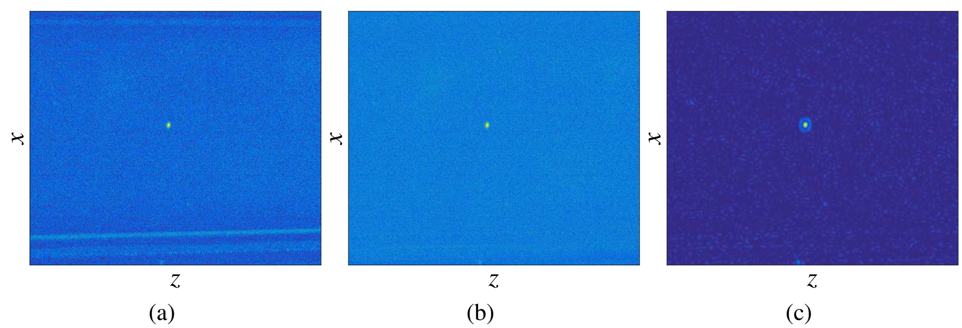

Figure 2: Image processing of a frame of a movie showing a single particle: (a) original image with color map applied, (b) subtraction of the background image obtained by averaging 200 frames, (c) convolution with the Laplacian of Gaussian filter. The particle is shown in bright yellow.

leading to an average width of $\overline{W} = 64\,\text{mm}$. The aspect ratio is defined as $\Gamma_{\text{exp}} = \overline{W}/H = 1.6$. Silicone oil with kinematic viscosity $\nu = 20\,\text{cSt}$ and density $\rho_\text{f} = 0.95\,\text{g/cm}^3$ at $T = 25\,^\circ\text{C}$ is used as the working fluid. The particles we employ are high-density polyethylene spheres with two different radii, $r = 2.0\,\text{mm}$ and $r = 0.6\,\text{mm}$. The particles are both nearly-neutrally buoyant. The larger particle is lighter with density $\rho_\text{p} = 0.947\,\text{g/cm}^3$ and the small one is heavier than the liquid with $\rho_\text{p} = 0.96\,\text{g/cm}^3$. In the following, we shall use the non-dimensional radius $a = r/H$ and the particle-to-fluid density ratio $\rho = \rho_\text{p}/\rho_\text{f}$.

A stereoscopic single particle tracking was performed by using two synchronized cameras which can capture the particle motion from two different viewpoints above the cavity. The three-dimensional position of the particle is reconstructed from its image projections captured by the two cameras using the 3D particle positioning algorithm detailed in Spinewine et al. (2003). The particle centroid in each 2D image plane can be determined by three steps shown in Fig. 2: (a) The original image is converted to a gray-scale image using a blue-to-yellow colormap, where the particle is identified as a bright yellow region. (b) From each frame, a background image obtained by averaging 200 consecutive frames, is subtracted. (c) After applying a convolution with the Laplacian of Gaussian filter the coordinates of the maximum response are identified as the centroid of the particle.

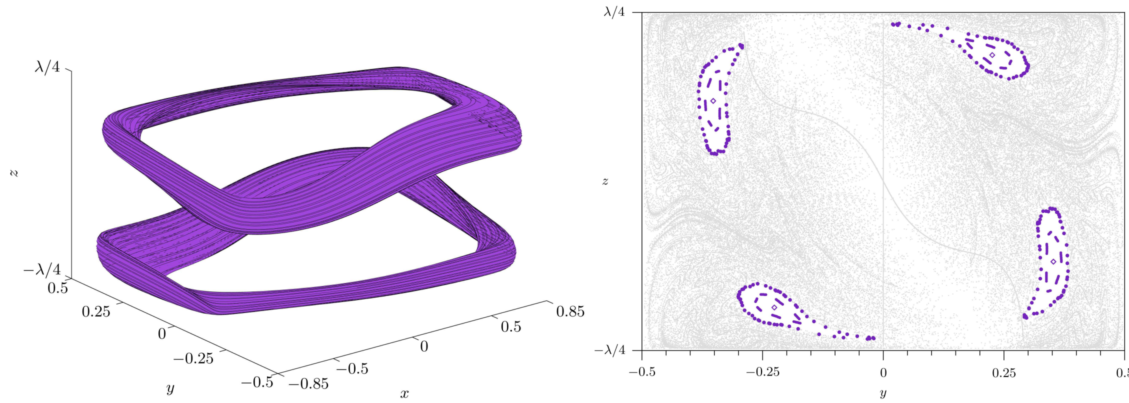

(a) (b)

Figure 3: Streamline topology of the flow in a two-sided lid-driven cavity at Re $= 400$ (Romanò et al., 2017): (a) Largest reconstructible KAM tori in an individual convection cell, (b) Poincaré section of 2500 streamlines on the plane $x = 0.5$. Purple islands outline the cross sections of the KAM surfaces. Gray dots represent Poincaré points of chaotic streamlines.

3 Results and discussion

Disregarding end-wall effects, the z-periodic steady three-dimensional convective cellular flow field in the two-sided lid-driven cavity is mirror symmetric with respect to all plane cell boundaries and point symmetric with respect to all cell centres (Kuhlmann et al., 1997; Blohm and Kuhlmann, 2002). At Re $= 400$ numerical simulations of Romanò et al. (2017) have revealed there exists a single pair of point-symmetric KAM tori inside of each individual convection cell which is immersed in a large chaotic region. Their result is reproduced in Fig. 3.

A neutrally buoyant finite-size particle which is initially advected in the chaotic region of the flow is eventually transported near one of the moving walls since the streamlines in the immediate vicinity of all walls are chaotic and the flow/transport can be assumed ergodic. Near the moving walls, the particle will be rapidly decelerated in wall-normal direction, as described above, after which it will essentially slide parallel to the moving wall. During the sliding phase, the distance Δ (in units of H) of the particle centroid from the moving wall remains nearly constant (Romanò and Kuhlmann, 2017) before it is released back to the bulk. The minimum distance of the particle centroid from the moving wall $\Delta = a + \delta$ comprises of the particle radius a and the lubrication-gap width δ between the particle's surface and the moving wall. In cases in which regular streamlines of a set of KAM tori approach the moving walls closer than Δ, the particle can be transported from the chaotic region to this regular region. The transfer process arises during the sliding phase, and repeated particle–boundary interactions can further focus the particle trajectory. Depending on the particle and flow properties a particle can be attracted to different attractors (Muldoon and Kuhlmann, 2013). The most striking ones are periodic or quasi-periodic orbits confined to the respective set of nested KAM tori. These orbits are nearly streamlines in the bulk which are connected near the boundary where the particle motion significantly deviates from the streamlines. In the present study, we consider Re $= 400$ and find periodic and quasi-periodic attractors for particles with $a = 0.05$, $\rho = 0.997$ and $a = 0.015$, $\rho = 1.01$, respectively.

3.1 Periodic attractor for a particle with $a = 0.05$ and $\rho = 0.997$

For Re $= \Omega R H/\nu = 400$ a particle with $a = 0.05$ and $\rho = 0.997$ is observed to be quite rapidly attracted to a limit cycle. The limit cycle is shown in blue in Fig. 4. For the selected flow and particle parameters the limit cycle nearly coincides with the closed streamline (red) inside of the KAM torus. The reason is the closed streamline for this particular case approaches the moving wall(s) with a minimum distance which nearly equals Δ. Due to repeated particle–boundary interactions, once the particle is captured inside of the KAM torus, it will settle very near the closed streamline.

To demonstrate the reproducibility of the particle attraction, regardless of its initial position, the experiment was repeated 40 times. At the beginning of each measurement, a random position for a single

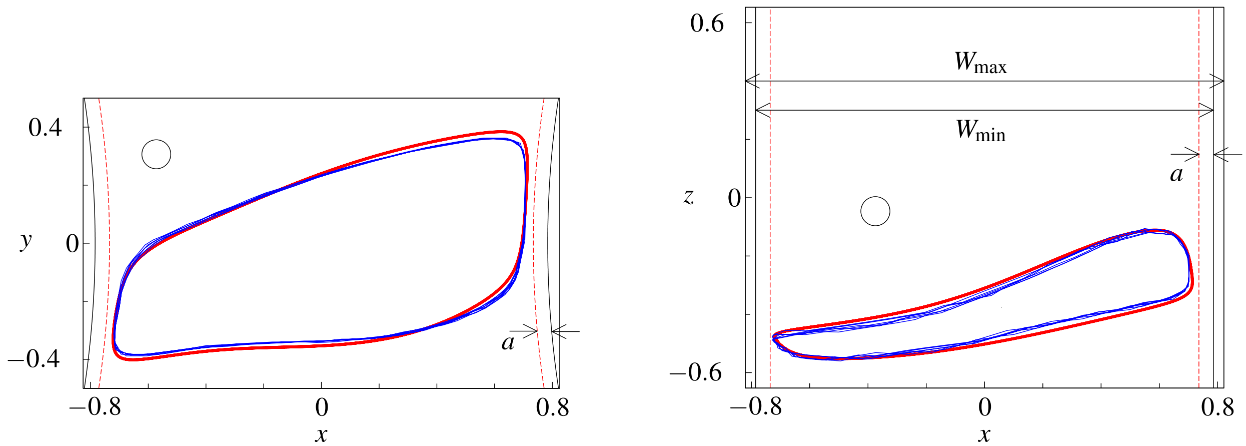

(a) (b)

Figure 4: Trajectory of the particle's centroid (blue) made of 15 revolutions about the limit cycle for $a = 0.05$. The trajectory was recorded 65 s after Re was set to 400. The closed streamline (red) is obtained by numerical simulation. Circles indicate the size of the particle. All length are given in units of H. (a) Projection to the (x,y) plane, (b) projection to the (x,z) plane.

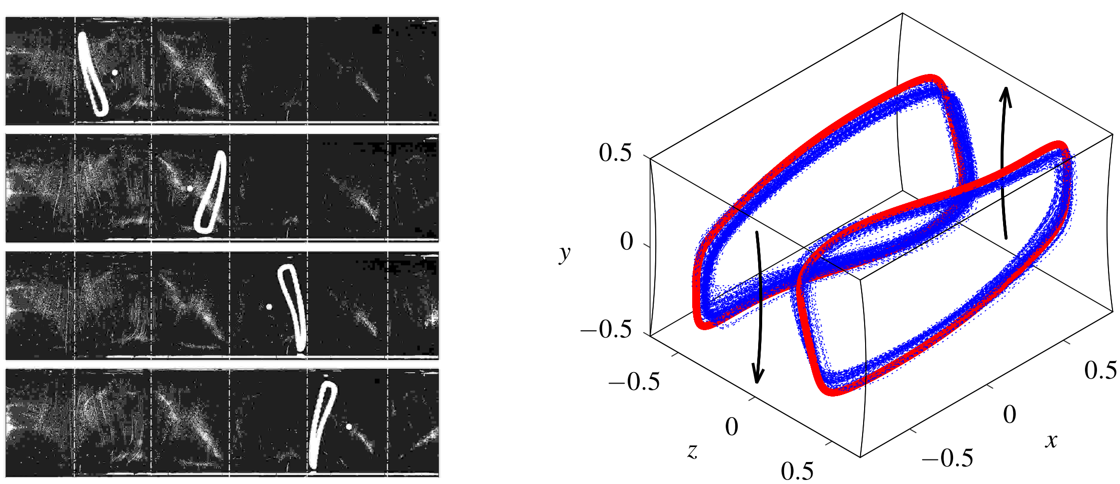

(a) (b)

Figure 5: (a) Long-time-exposure images from top view showing the (x,z) plane. The four images show the particle being trapped in different convective cells (indicated by dashed lines) which can be identified by fine streaklines made by small aluminium flakes. (b) 40 Particle trajectories (blue) during approximately 15 revolutions each and two closed streamlines (red) for $a = 0.05$ and $\mathrm{Re} = 400$.

particle is realized by setting the Reynolds number to $\mathrm{Re} = 1600$ which drives the flow into a fully time-dependent chaotic state. This chaotic flow state must be strictly distinguished from Lagrangian chaos with *steady* streamlines. After 60 s the Reynolds number was linearly decreased within 2 s to $\mathrm{Re} = 400$. For each realization of the experiment the particle is found to settle in one of the periodic convection cells, as shown in Fig. 5(a). Since the flow is spatially periodic, all closed streamlines and particle attractors can be mapped to the two generic line-like attractors of a single cell. All trajectories shown have been recorded for 40 s, starting 65 s after $\mathrm{Re} = 400$ was reached. The duration of the record corresponds to approximately 15 revolutions about the limit cycle.

Figure 5(b) shows the superposition of all 40 single-particles trajectories (blue) mapped to the generic convection cell. For comparison, the two closed streamlines inside of the two mirror symmetric sets of KAM tori (obtained numerically) are shown in red. The shapes and locations of the particle attractors match very well with the closed streamlines.

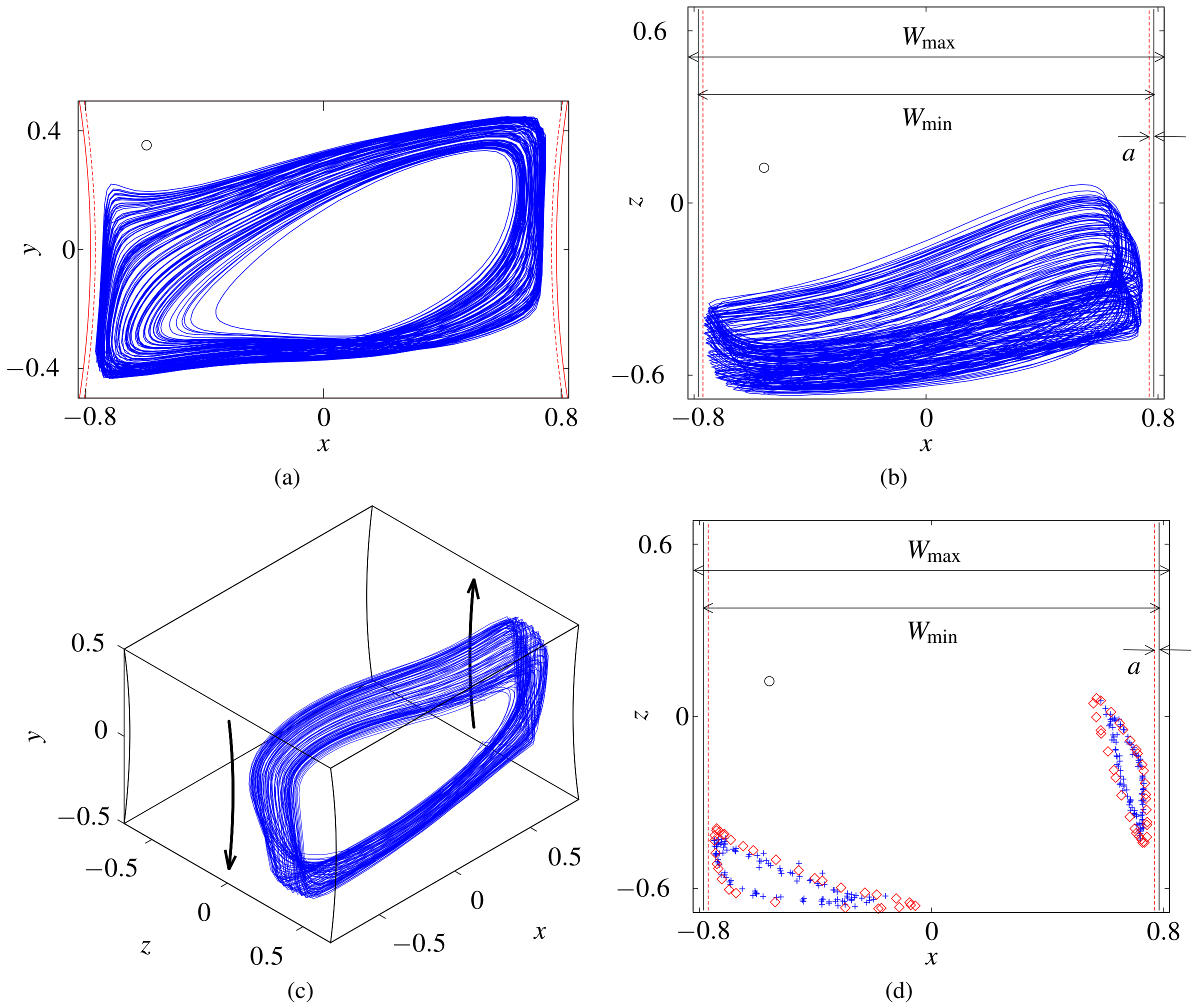

Figure 6: Trajectory of the centroid of a single particle making 100 revolutions for $a = 0.015$ and $\mathrm{Re} = 400$. The record started 2 min after $\mathrm{Re} = 400$ was reached. Circles indicate the particle size. Shown are projections of the particle's centroid to the (x, y) (a) and (x, z) (b) planes, as well as a three-dimensional view (c). A Poincaré section on the plane $y = 0$ (d) reveals the tubular structure of the attractor (blue) which compares well with a KAM torus (red).

3.2 Quasi-periodic tubular attractor for a particle with $a = 0.015$ and $\rho = 1.01$

For the particle with radius $a = 0.015$ and $\rho = 1.01$ a tubular attractor is found. Figure 6 shows the trajectory during 220 s which corresponds to 100 revolutions about the main vortex structure in the cavity. The trajectory was recorded starting 2 min after $\mathrm{Re} = 400$ was reached. The smaller size of the particle leads to a smaller value of Δ. Therefore, the particle is transferred from the chaotic to the regular region at a smaller distance Δ from the moving boundaries than in case of the larger particle discussed in Sec. 3.1. Hence, once captured in the regular region, the particle is essentially advected on KAM tori, between successive particle–boundary interactions, and is finally transferred to a tubular structure which is very similar to the specific KAM torus which approaches the moving boundary up to the distance Δ. The mechanism of attraction has been explained by Hofmann and Kuhlmann (2011). After attraction to the tubular structure, the particle performs a quasi-periodic motion, very similar as a streamline on the corresponding KAM stream tube. A comparison between the outermost KAM torus, obtained numerically, and the particle trajectory is made in Fig. 6(d) which shows a Poincaré section on the plane $y = 0$. The position and shape of both tori are very similar.

4 Conclusion

Attractors for the motion of neutrally-buoyant finite-size particles have been found in the steady incompressible three-dimensional flow in a two-sided lid-driven cavity. The shape and location of the particle attractors are in good agreement with periodic or quasi-periodic streamlines of the flow which were obtained numerically. The rapid attraction can be explained by the particle–boundary interaction for finite-size particles. While particle inertia is not necessary to explain the results, very small inertial forces exist even for the present small density mismatch of less than 1% between the particle and the fluid. Therefore, inertia may still play a certain role in the dynamical evolution on very long time scales. It would thus be interesting to investigate the particle behaviour on much longer time scales to clarify the influence of the density ratio on the resulting attractors.

References

Albensoeder S and Kuhlmann HC (2002) Linear stability of rectangular cavity flows driven by anti-parallel motion of two facing walls. *Journal of Fluid Mechanics* 458:153–180

Blohm CH and Kuhlmann HC (2002) The two-sided lid-driven cavity: experiments on stationary and time-dependent flows. *Journal of Fluid Mechanics* 450:67–95

Hofmann E and Kuhlmann HC (2011) Particle accumulation on periodic orbits by repeated free surface collisions. *Physics of Fluids* 23:072106

Kuhlmann HC, Romanò F, Wu H, and Albensoeder S (2016) Particle-motion attractors due to particle–boundary interaction in incompressible steady three-dimensional flows. in G Ivey, T Zhou, N Jones, and S Draper, editors, *The 20th Australasian Fluid Mechanics Conference*. pages 102, Paper no. 449. Australasian Fluid Mechanics Society

Kuhlmann HC, Wanschura M, and Rath HJ (1997) Flow in two-sided lid-driven cavities: non-uniqueness, instabilities, and cellular structures. *Journal of Fluid Mechanics* 336:267–299

Mukin RV and Kuhlmann HC (2013) Topology of hydrothermal waves in liquid bridges and dissipative structures of transported particles. *Physical Review E* 88:053016

Muldoon FH and Kuhlmann HC (2013) Coherent particulate structures by boundary interaction of small particles in confined periodic flows. *Physica D: Nonlinear Phenomena* 253:40–65

Ottino JM (1989) *The kinematics of mixing: stretching, chaos, and transport*. volume 3. Cambridge University Press

Romanò F, Albensoeder S, and Kuhlmann HC (2017) Topology of three-dimensional steady cellular flow in a two-sided anti-parallel lid-driven cavity. *Journal of Fluid Mechanics* 826:302–334

Romanò F and Kuhlmann HC (2016) Numerical investigation of the interaction of a finite-size particle with a tangentially moving boundary. *International Journal of Heat and Fluid Flow* 62 Part A:75–82

Romanò F and Kuhlmann HC (2017) Particle–boundary interaction in a shear-driven cavity flow. *Theoretical and Computational Fluid Dynamics* 31:427–445

Spinewine B, Capart H, Larcher M, and Zech Y (2003) Three-dimensional Voronoï imaging methods for the measurement of near-wall particulate flows. *Experiments in Fluids* 34:227–241